Non-parametric Analysis of Hyperpolarized Dynamic ^{13}C Lactate Imaging in a Transgenic Mouse Model of Prostate Cancer

J. M. Lupo[1], A. P. Chen[1], C. H. Cunningham[2], R. Bok[1], J. Kurhanewicz[1], D. B. Vigneron[1], and S. J. Nelson[1]

[1]Department of Radiology, University of California, San Francisco, California, United States, [2]Department of Medical Biophysics, Sunnybrook Health Sciences Centre, Toronto, Canada

Introduction

Prior studies have shown that serial MRS acquisitions can detect the dynamic uptake of hyperpolarized ^{13}C-pyruvate and its metabolic conversion to ^{13}C-lactate, ^{13}C-alanine, and ^{13}C-bicarbonate *in vivo* (1-3). Recently, hyperpolarized ^{13}C-pyruvate studies of a transgenic prostate cancer mode using rapid 3D MRSI techniques demonstrated significantly higher levels of ^{13}C-lactate in tumor voxels compared to non-cancer regions and that the ^{13}C-lactate/(total ^{13}C) ratios correlated positively with disease progression (3,4). These 3D MRSI acquisitions were acquired in 10-14s starting ~30s after the initiation of the hyperpolarized ^{13}C-pyruvate and provided valuable spatial information but provided no temporal dynamic data. In this study we obtained serial 3D images of ^{13}C-lactate with a temporal resolution of 5s using a pulse sequence that incorporates spectral-spatial rf pulses and a rapid echo-planar readout to track the time course of ^{13}C lactate *in vivo* after injection of pre-polarized ^{13}C-pyruvate. The goal of this study was to determine the feasibility of using dynamic ^{13}C lactate imaging for investigating prostate cancer metabolism *in vivo*.

Methods

Animals and MR studies: Seven TRansgenic Adenocarsinoma of Mouse Prostate (TRAMP) mice with varying degrees of disease development were scanned on a GE 3T MR system, using a custom designed ^{1}H/^{13}C dual tuned mouse coil. A flyback echo-planar pulse sequence was used to acquire data from a 3D volume (10 cm FOV, 6.4 cm thick slab) with a 32x32x16 spatial matrix (0.039cc voxel resolution) in 3.5s. The sequence incorporated a spectral-spatial excitation pulse (180 Hz pass band, 440 Hz stop band) that selectively excited ^{13}C-lactate while keeping the magnetization of ^{13}C-pyruvate along M_z. Imaging began at the same time as the injection of a 350µl solution of pre-polarized $^{13}C_1$-pyruvate via DNP. 3D lactate images were acquired with 5s temporal resolution for 100s (20 temporal time points).

Data Analysis: The peak lactate signal height (PH), full-width half max of ^{13}C-lactate (FWHM), and time to the peak ^{13}C-lactate signal (TTP) were calculated from the dynamic data on a voxel by voxel basis. Median and/or maximum values of each parameter were determined for regions of tumor and kidney. The peak lactate signal height was normalized by both the percent polarization and the amount injected. Statistical significance of differences between tumor and kidney were determined through the use of a Wilcoxon signed rank test.

Results & Discussion

Table 1 shows the parameters extracted from the ^{13}C dynamic imaging studies for both tumor and kidney regions of interest from mice with different degrees of disease progression. The shape of the lactate curve varied spatially within the tumor, reflecting heterogeneity of the disease as illustrated by the representative data in Figure 1 from one mouse with advanced disease (top) and one mouse with a tumor at an earlier degree of progression (bottom). Elevated PH and shorter widths were observed within the tumor for mice with more advanced tumors compared to those with early stage of disease development (Figure 1), although lower ^{13}C lactate SNR in the mice with early stage disease may have limited the accuracy of the FWHM measurements. The shapes of the dynamic lactate curves differed between regions of the tumor and kidney in these mice (Figure 2). The kidneys demonstrated 10-15s shorter TTP, 3-fold narrower FWHM, and higher PH values compared to tumor.

Conclusions

This study demonstrated the feasibility of using 3D ^{13}C dynamic lactate imaging to characterize lactate metabolism in vivo at high spatial and temporal resolution in a transgenic mouse model of prostate cancer. Non-parametric values obtained from the ^{13}C lactate dynamic curves demonstrated differences within individual tumors as well as between tumors with different levels of disease progression. This new acquisition offers novel spatially resolved dynamic data of ^{13}C lactate that was not applied in previous studies (1-3), and may improve our understanding of *in vivo* lactate metabolism in these disease models. Further studies will investigate whether the differences that were seen in the ^{13}C lactate dynamic data were related to blood supply, substrate uptake, and/or the rate of conversion of pyruvate to lactate.

Table 1.	*Disease*	**Median Peak Height**		**Max Peak Height**		**Median FWHM (s)**		**Median TTP (s)**		**No. of Voxels**	
Mouse	*Development**	*tumor*	*kidney*	*tumor*	*kidney*	*tumor*	*kidney*	*tumor*	*kidney*	*tumor*	*kidney*
1	Early	23.33	97.29	38.89	170.69	13.5	5	25	15	8	5
2	Early	17.48	16.57	24.97	76.67	16.5	14	15	15	8	5
3	Early	19.09	58.70	38.77	100.04	15	4	30	20	13	4
4	Early	17.23	60.47	20.98	127.35	17	4	35	20	8	7
5	Late	32.22	183.97	151.90	285.16	7	4	30	20	25	4
6	Late	50.31	94.39	77.58	162.12	7	5	25	15	11	5
7	Late	32.93	69.52	61.33	124.84	7	4	30	15	15	4
Median		***23.3±12.0***	***69.5±52.0***	***38.9±45.5***	***127.4±68.1***	***13.5±4.7***	***4.0±3.7***	***30.0±6.4***	***15.0±2.7***	***11.0±6.1***	***5.0±1.1***
P-Value		*P = 0.031*		*P = 0.016*		*P = 0.016*		*P = 0.031*		*P = 0.016*	

* The tumor progression was classified as early or late using MRI/^{13}C MRSI data that were acquired in the same exam (4).

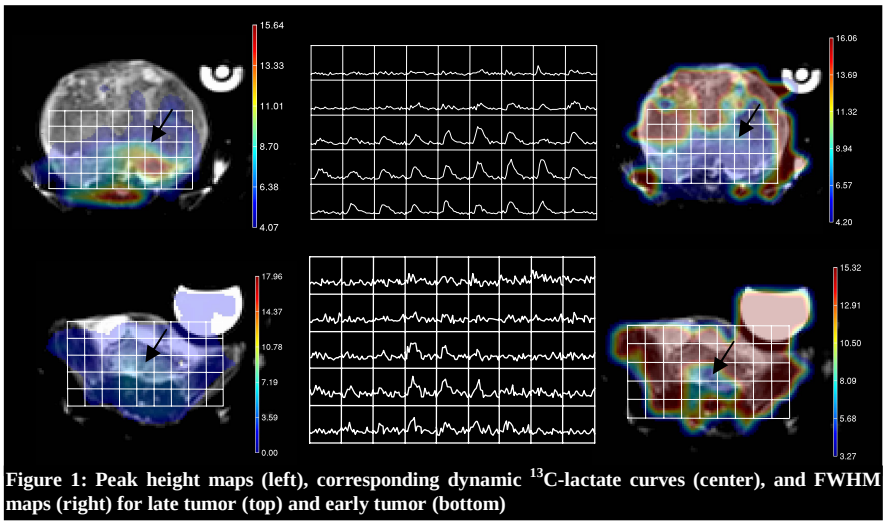

Figure 1: Peak height maps (left), corresponding dynamic ^{13}C-lactate curves (center), and FWHM maps (right) for late tumor (top) and early tumor (bottom)

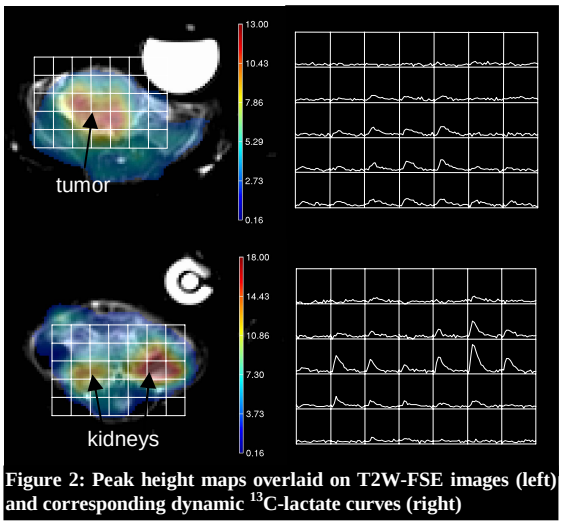

Figure 2: Peak height maps overlaid on T2W-FSE images (left) and corresponding dynamic ^{13}C-lactate curves (right)

References & Acknowledgements

(1) Golman K et. al. PNAS, 2006; 103(30):11270-11275. (2) Kohler SJ et. al. Magn Reson Med, 2007;58(1):65-69. (3) Chen AP et. al. Magn Reson Med, in press. (4) Albers M et. al. In Proc. ISMRM annual meeting 2007, Berlin; #367. This research was supported by grants R21-EB005363, R01-CA111291, R01-EB007588.